Supplementary Material

Crystal structure evolution via operando neutron diffraction during long-term cycling of customized 5 V full Li-ion cylindrical cells LiNi$_{0.5}$Mn$_{1.5}$O$_4$ vs. graphite

Lucien Boulet-Roblin[1+], Denis Sheptyakov[2+], Philippe Borel[3], Cécile Tessier[3], Petr Novák[1], Claire Villevieille[1*]

Comparison between the neutron diffraction patterns of a commercial cell and our cylindrical cell
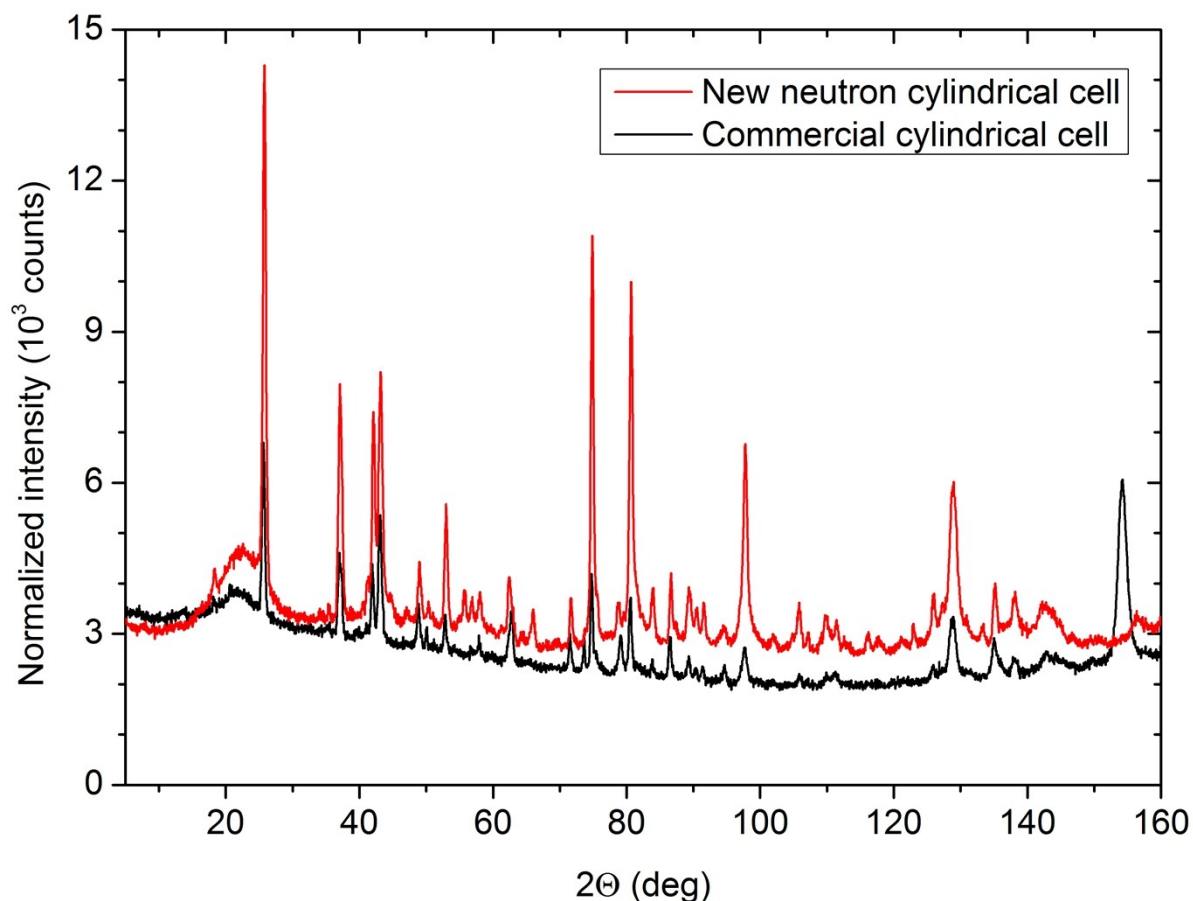
Figure S1: Neutron powder diffraction patterns of d-LNMO vs. graphite cell recorded with commercial cell and new neutron cell design. Both datasets were accumulated in identical instrument settings during approximately 1.5 hours, and than explicitly normalized to identical neutron monitor counts. The diffraction intensity, and peak-to-background ratio in the pattern of a new neutron cylindrical cell is a lot higher. Some extra coherent diffraction peaks in the pattern of the commercial cell, including the strong peak at ~154 deg, are due to the diffraction on the iron casing of the cell.

Rietveld refinement based on neutron powder diffraction data obtained from a cell prior to cycling at OCV.

Table S1: Crystallographic data obtained from the Rietveld refinement of d-LNMO and graphite recorded prior to cycling (30 min of acquisition).

d-LNMO: refined composition: $LiNi_{0.51(1)}Mn_{1.49(1)}O_4$			
Space group: *Fd-3m (#227)*, Z=8, a = 8.1705 (8) Å,			
the sites of Li and O assumed 100% occupied.			
Atom	Wyckoff site		
Ni/Mn	*16d (1/2,1/2,1/2)*	occ Ni:Mn (%)	25.5 (4) : 74.5 (4)
		B_{iso} (Å^2)[i]	0.4
Li	*8a (1/8,1/8,1/8)*	B_{iso} (Å^2)[ii]	0.52 (9)
O	*32e (x,x,x)*	x	0.2640 (2)
		B_{iso} (Å^2)	0.26 (5)

Graphite, Space Group P6$_3$/mmc, Z=2, a = 2.4623 (2), c = 6.7141 (7)			
Atom	Wyckoff site		
C1	*2b* (0,0,1/4); and	$B_{iso,}$ (Å^2) [iii]	0.45 (3)
C2	*2c* (1/3,2/3,1/4);		

[i] B_{iso} parameter for Ni/Mn was fixed in this refinement. Given the opposite signs of the bound coherent neutron scattering lengths of Ni (10.3 fm) and Mn (-3.73 fm), and the refined proportion of Ni and Mn in the *16d* site (close to 1:3), the average scattering length of cation in this site is very close to 0 (under assumption of the correctly refined proportions, the average $b_{Ni/Mn} \approx$ -0.15 fm). While the partial Ni/Mn occupancy of the position is a very precisely refined parameter, and there are no coordinates to be refined (this is a special position), the B_{iso} values are on the contrary, a very poorly determined parameter in such refinement. For this reason, the B_{iso} value for Ni/Mn atoms was fixed to a reasonable value of 0.4 Å^2.

[ii] B_{iso} for Li atom was constrained to be exactly twice larger than that refined for oxygen, reason being a rather poor contribution of Li to the total intensity, and thus not sufficiently high reliability of its thermal parameters individual refinement.

[iii] B_{iso} values for both carbon atoms in graphite were refined with constraint to equality.

Rietveld refinement based on the neutron powder diffraction data collected ex-situ on the material of the half-charged cathode.
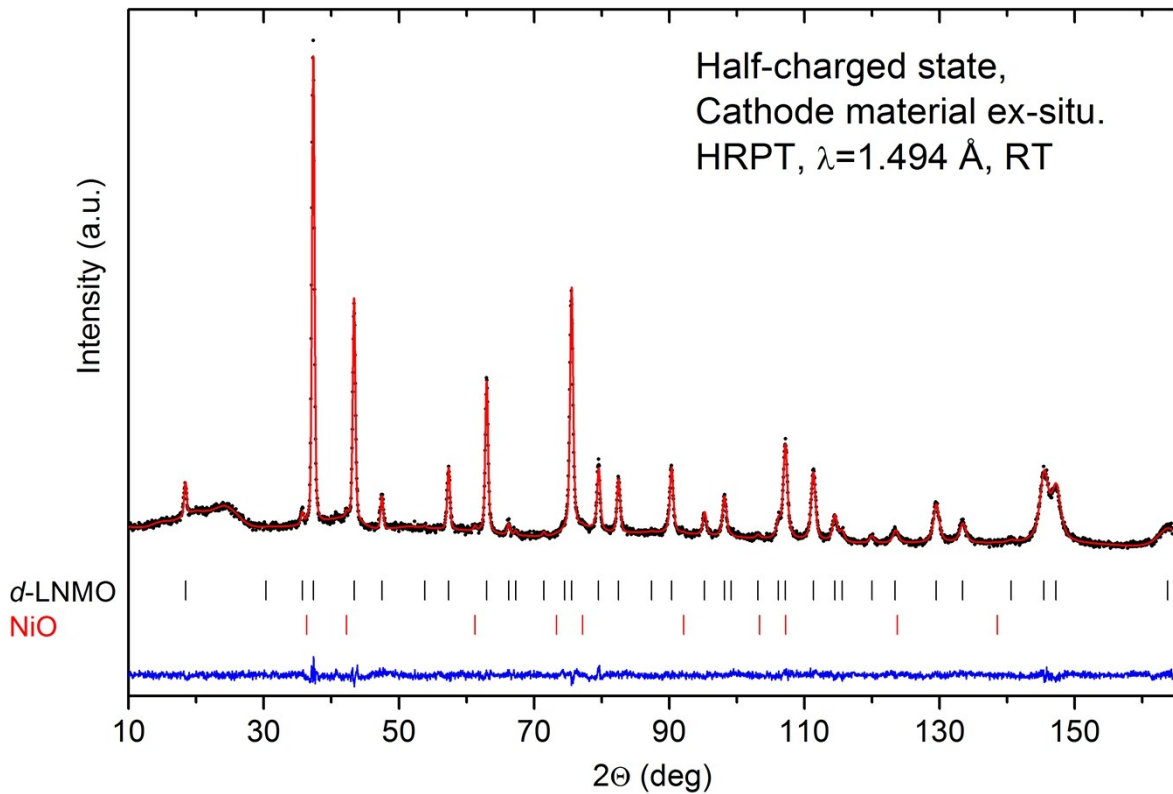
Figure S2: Rietveld refinement based on the ex-situ NPD pattern of material of the half-charged cathode. Experimental points, calculated profile and difference curve are shown, the rows of ticks below the graphs correspond to the calculated positions of the diffraction peaks of the contributing phases, in the order from top to bottom: d-LNMO, and NiO impurity (wt. 0.5%).

Table S2: Crystallographic data obtained from the Rietveld refinement based on the ex-situ NPD pattern of material of the half-charged cathode.

d-LNMO: refined composition: $Li_{0.39(2)}Ni_{0.46(1)}Mn_{1.54(1)}O_4$			
Space group: *Fd-3m (#227)*, Z=8, a = 8.0914(3) Å,			
the O position (*32e* site) assumed 100% occupied.			
Atom	Wyckoff site		
Ni/Mn	*16d (1/2,1/2,1/2)*	occ Ni:Mn (%)	23.1 (3) : 76.9(3)
		B_{iso} (Å^2)[iv]	0.4
Li	*8a (1/8,1/8,1/8)*	frac. occ.	0.39 (2)
		B_{iso} (Å^2)[v]	1.20 (2)
O	*32e (x,x,x)*	x	0.2635 (1)
		B_{iso} (Å^2)	0.60 (1)

[iv] B_{iso} parameter for Ni/Mn was fixed in this refinement. Given the opposite signs of the bound coherent neutron scattering lengths of Ni (10.3 fm) and Mn (-3.73 fm), and the refined proportion of Ni and Mn in the *16d* site (close to 1:3), the average scattering length of cation in this site is very close to 0 (under assumption of the correctly refined proportions, the average $b_{Ni/Mn} \approx -0.49$ fm). While the partial Ni/Mn occupancy of the position is a very precisely refined parameter, and there are no coordinates to be refined (this is a special position), the B_{iso} values are on the contrary, a very poorly determined parameter in such refinement. For this reason, the B_{iso} value for Ni/Mn atoms was fixed to a reasonable value of 0.4 Å^2.

[v] B_{iso} for Li atom was constrained to be exactly twice larger than that refined for oxygen. Li itself being a relatively weak neutron scatterer (-1.90 fm), produces yet weaker scattering when its position is less than half-filled, as in this case of the half-delithiated d-LNMO material. The refinement of the B_{iso} thermal parameter becomes hereby less reliable, so an assumption was needed to be made, and an estimation of a twice larger B_{iso} as compared to that of oxygen was chosen as supposedly reasonable.

Rietveld refinement based on the neutron powder diffraction data collected ex-situ on the material of the completely charged (delithiated) cathode.
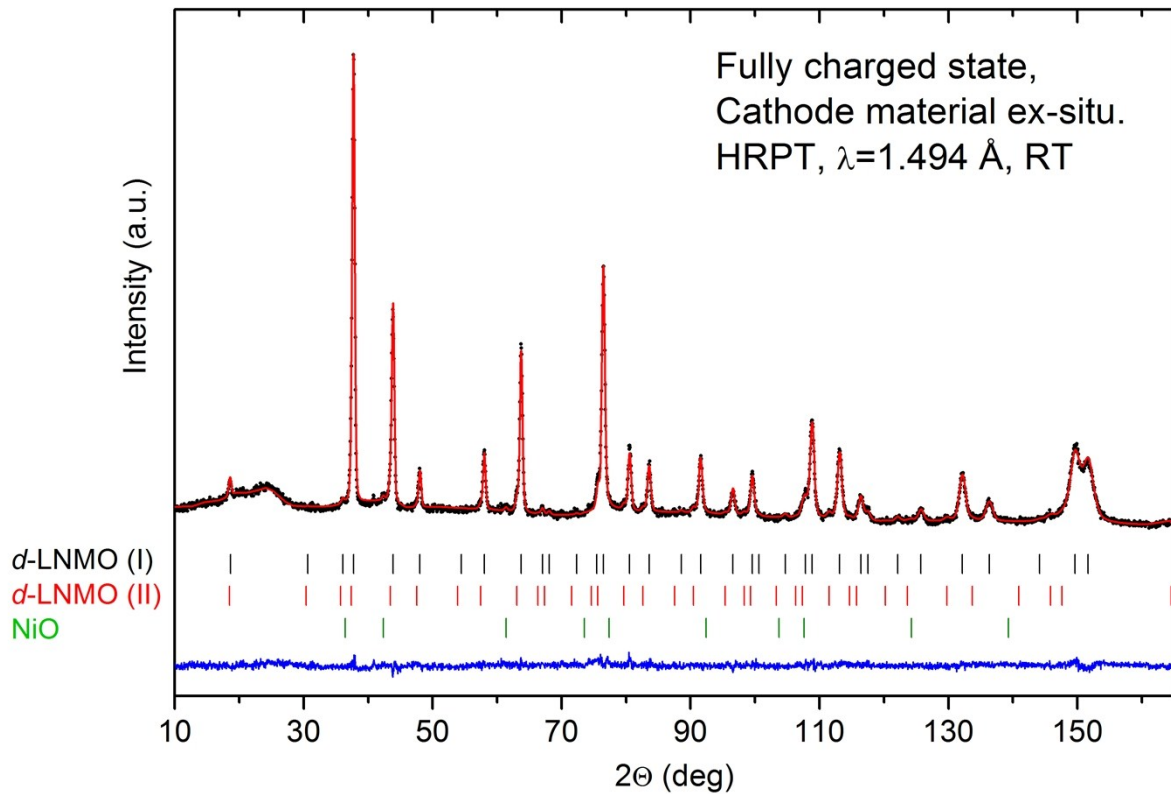
Figure S3: Rietveld refinement based on the ex-situ NPD pattern of material of the half-charged cathode. Experimental points, calculated profile and difference curve are shown, the rows of ticks below the graphs correspond to the calculated positions of the diffraction peaks of the contributing phases, in the order from top to bottom: Li-free d-LNMO (I) phase (wt. ~91.9%), Li-bearing d-LNMO (II) phase (wt. ~7.6%), and NiO impurity (wt. ~0.5%).

Table S3: Crystallographic data obtained from the Rietveld refinement of based on the ex-situ NPD pattern of material of the completely charged cathode. Apart from the NiO impurity (wt. ~0.5%), and a minor admixture of the "half-delithiated" d-LNMO phase (wt. ~7.6%, the crystal structure parameters of which were fixed to those listed in the Table S2), the major phase constituting the cathode material is a practically Li-free d-LNMO phase. The refined parameters in this Table refer to the parameters of exactly this, practically Li-free phase.

d-LNMO: refined composition: $Li_{0.00(2)}Ni_{0.46(1)}Mn_{1.54(1)}O_4$			
Space group: *Fd-3m (#227)*, Z=8, a = 8.0068(3) Å,			
the O position (*32e* site) assumed 100% occupied.			
Atom	Wyckoff site		
Ni/Mn	*16d (1/2,1/2,1/2)*	occ Ni:Mn (%)	23.1 (3) : 76.9(3)
		B_{iso} (Å^2)[vi]	0.4
Li	*8a (1/8,1/8,1/8)*	frac. occ. [vii]	0.00 (4)
O	*32e (x,x,x)*	x	0.2628 (1)
		B_{iso} (Å^2)	0.46 (1)

[vi] B_{iso} parameter for Ni/Mn was fixed in this refinement. Given the opposite signs of the bound coherent neutron scattering lengths of Ni (10.3 fm) and Mn (-3.73 fm), and the refined proportion of Ni and Mn in the *16d* site (close to 1:3), the average scattering length of cation in this site is very close to 0 (under assumption of the correctly refined proportions, the average $b_{Ni/Mn}$≈-0.49 fm). While the partial Ni/Mn occupancy of the position is a very precisely refined parameter, and there are no coordinates to be refined (this is a special position), the B_{iso} values are on the contrary, a very poorly determined parameter in such refinement. For this reason, the B_{iso} value for Ni/Mn atoms was fixed to a reasonable value of 0.4 Å^2.

[vii] The fractional occupancy of Li position was refined under a constraint assuming the B_{iso} for Li atom to be exactly twice larger than that refined for oxygen.

Evolution of the first discharge of graphite using operando neutron diffraction
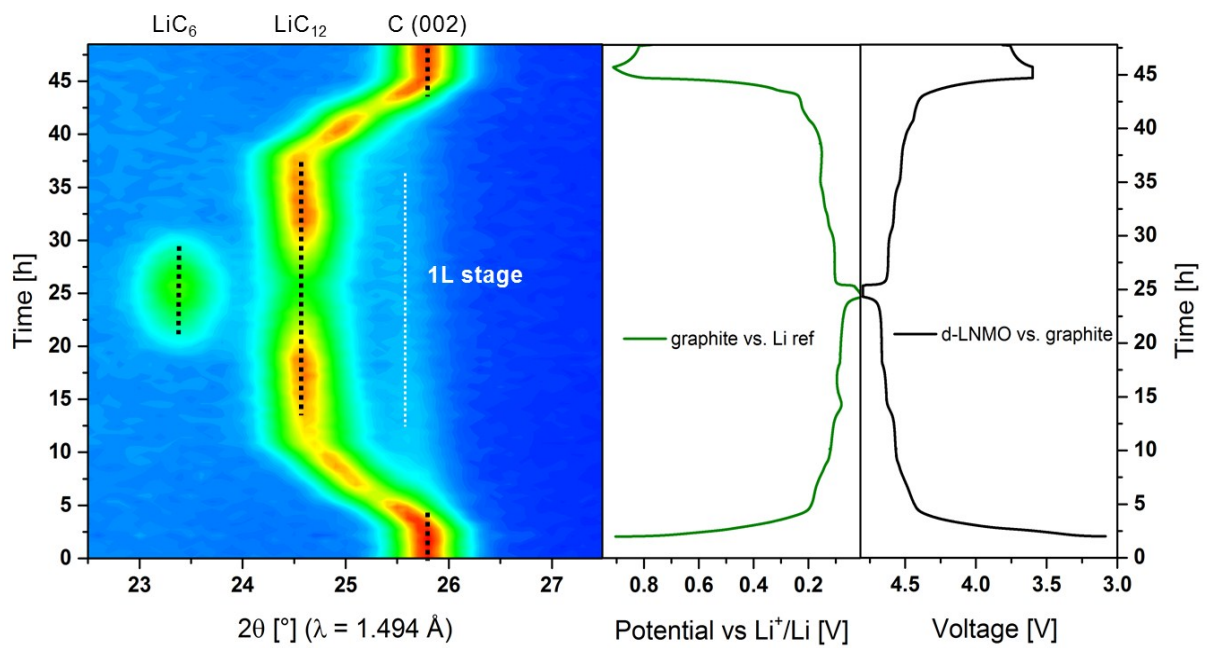
Figure S4 Contour plot representation of an operando NPD measurement of the first charge of d-LNMO vs graphite cylindrical cell: (left) the (002) graphite reflection is plotted, (right) the galvanostatic cycle of graphite vs Li ref or d-LNMO.

Rietveld refinement based on the NPD data obtained from the charged anode material
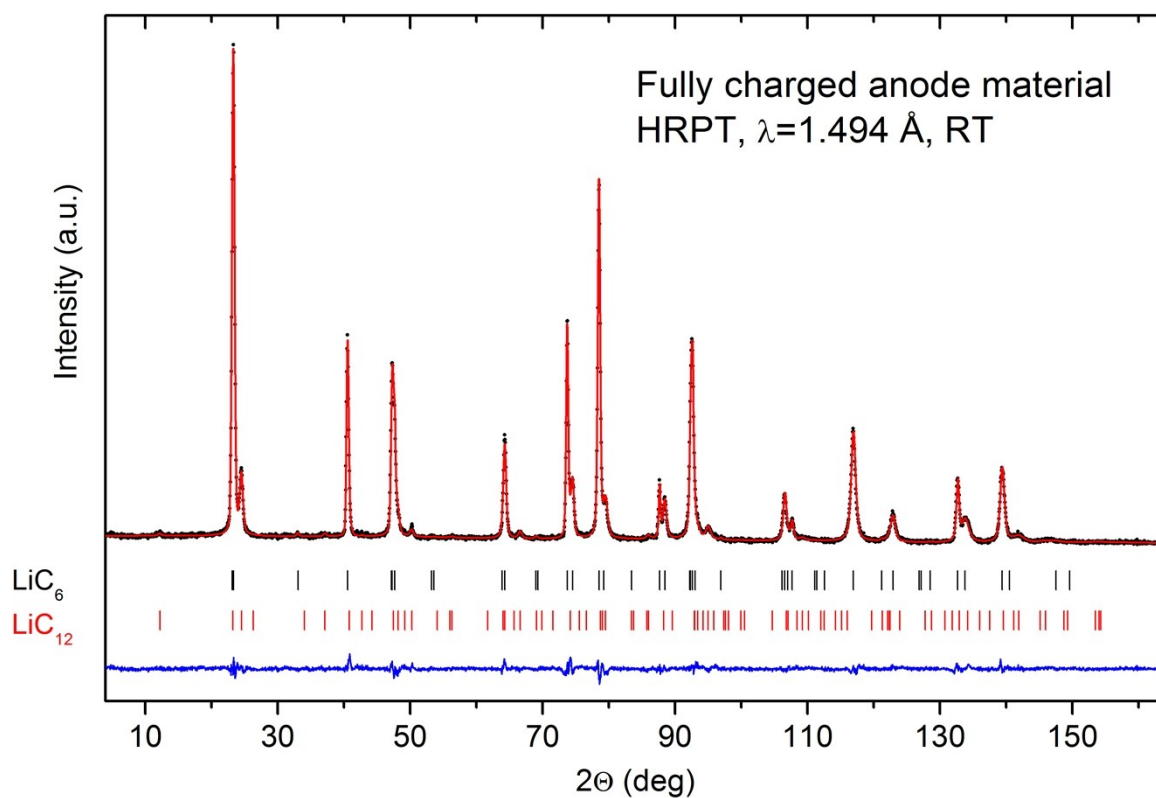
Figure S5: Rietveld refinement based on the ex-situ NPD pattern of material of the charged anode. Experimental points, calculated profile and difference curve are shown, the rows of ticks below the graphs correspond to the calculated positions of the diffraction peaks of the contributing phases, in the order from top to bottom: major phase LiC$_6$ (wt. ~86.0(6)%), and LiC$_{12}$ minor phase (wt. ~14.0(3)%).

Table S4: Crystallographic data obtained after Rietveld refinement of the fully-charged graphite electrode. Refined parameters are indicated in brown.

$Li_{\sim0.76(3)}C_6$ (wt. ~86%), Space Group $P6/mmm$, Z=1, a = 4.3165(2), c = 3.7024(2)			
Atom	Wyckoff site		
C	*6k (x,0,1/2);*	x	0.3334 (8)
		$B_{iso,}$ ($Å^2$) [viii]	0.42 (2)
Li	*1a (0,0,0)*	frac. occ.	0.76 (3)
		$B_{iso,}$ ($Å^2$) [ix]	0.84 (4)

$Li_{\sim1}C_{12}$ (wt. ~14%), Space Group $P6/mmm$, Z=1, a = 4.2924(4), c = 7.0444(7)			
Atom	Wyckoff site		
C	*12n (x,0,z);*	x	0.337 (6)
		z	0.2333 (5)
		$B_{iso,}$ ($Å^2$) [viii]	0.42 (2)
Li	*1a (0,0,0)*	frac. occ.	1.07 (18)
		$B_{iso,}$ ($Å^2$) [ix]	0.84 (4)

[viii] B_{iso} values for carbon atoms in both phases were refined with constraint to equality.

[ix] B_{iso} for Li atoms in both phases were constrained to be exactly twice larger than that refined for carbon atoms.

After 100 cycles
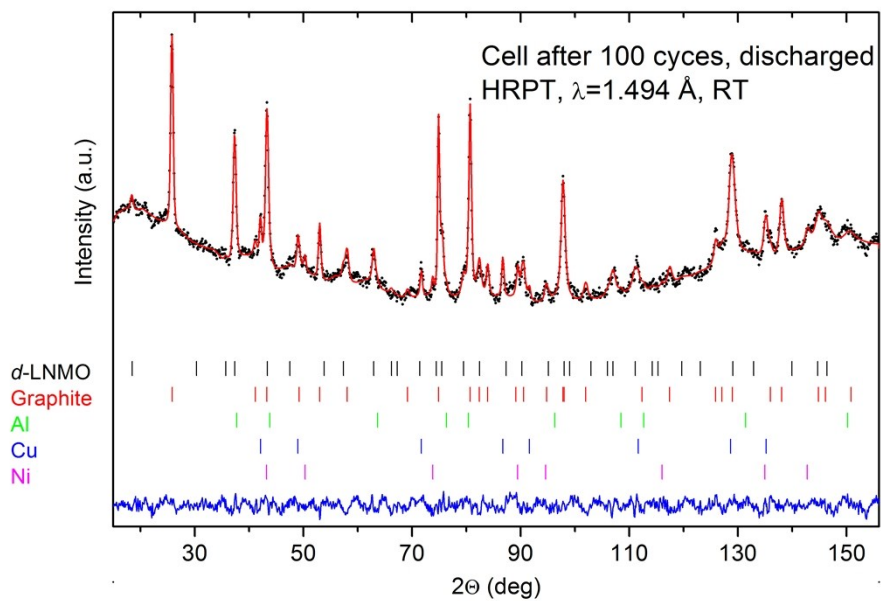
Figure S6: Rietveld refinement based on the NPD pattern of the d-LNMO vs graphite cylindrical cell after 100 cycles (discharged cell, 120 min of acquisition). Experimental points, calculated profile and difference curve are shown, the rows of ticks below the graphs correspond to the calculated positions of the diffraction peaks of the contributing phases (order from top to bottom: d-LNMO, graphite, Al, Cu, Ni).
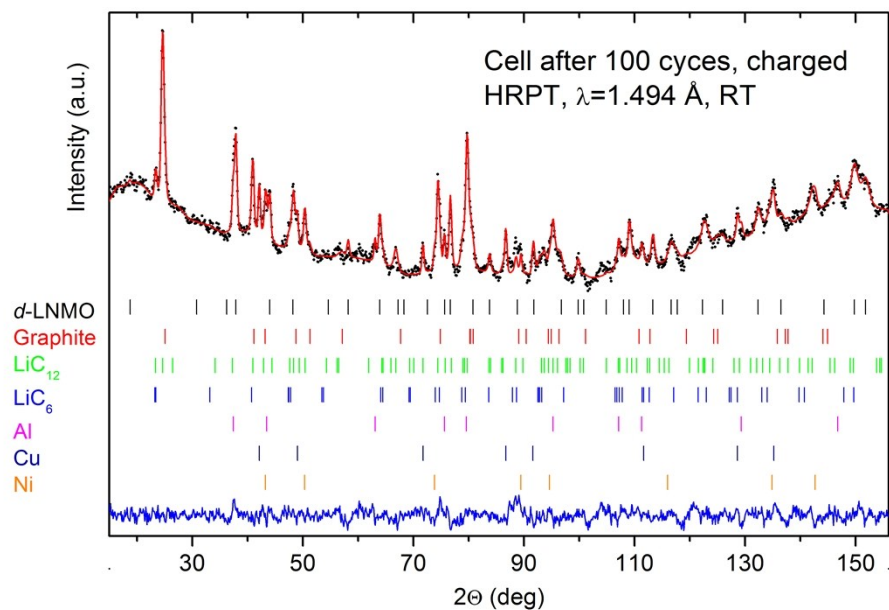
Figure S7: Rietveld refinement based on the NPD of the d-LNMO vs graphite cylindrical cell after 100 cycles (charged cell, 120 min of acquisition). Experimental points, calculated profile and difference curve are shown, the rows of ticks below the graphs correspond to the calculated positions of the diffraction peaks of the contributing phases (order from top to bottom: d-LNMO, graphite, LiC₁₂, LiC₆, Al, Cu, Ni).
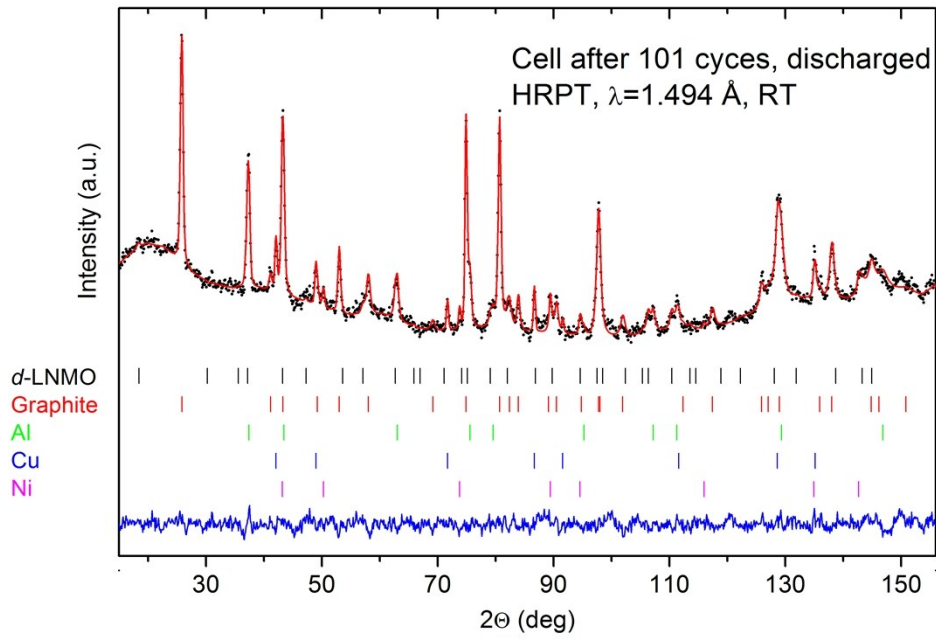
Figure S8: Rietveld refinement based on the NPD of the d-LNMO vs graphite cylindrical cell after 101 cycles (discharged cell, 80 min of acquisition). Experimental points, calculated profile and difference curve are shown, the rows of ticks below the graphs correspond to the calculated positions of the diffraction peaks of the contributing phases (order from top to bottom: d-LNMO, graphite, Al, Cu, Ni).
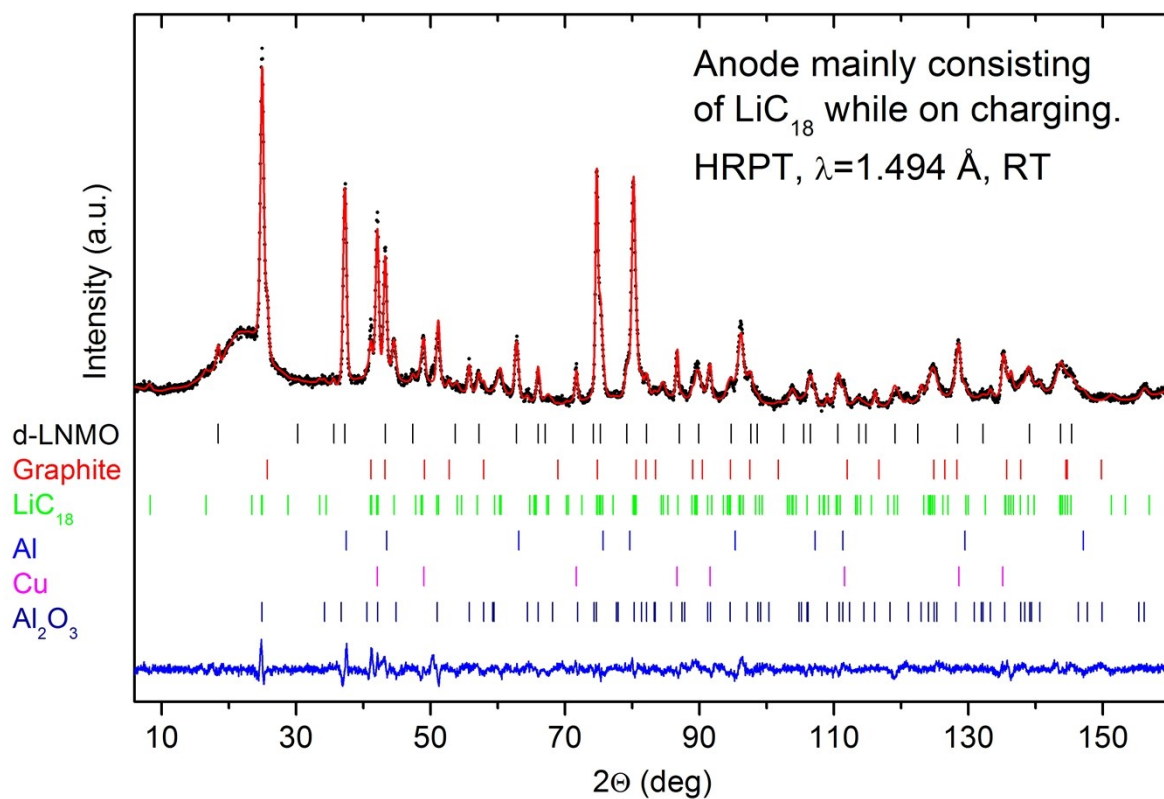
Figure S9. Rietveld refinement on the NPD data extracted for exactly the time when LiC$_{18}$ phase was dominating material in anode material, during the charging branch of the cycle.). Experimental points, calculated profile and difference curve are shown, the rows of ticks below the graphs correspond to the calculated positions of the diffraction peaks of the contributing phases (order from top to bottom: d-LNMO, graphite, Al, Cu, Ni).
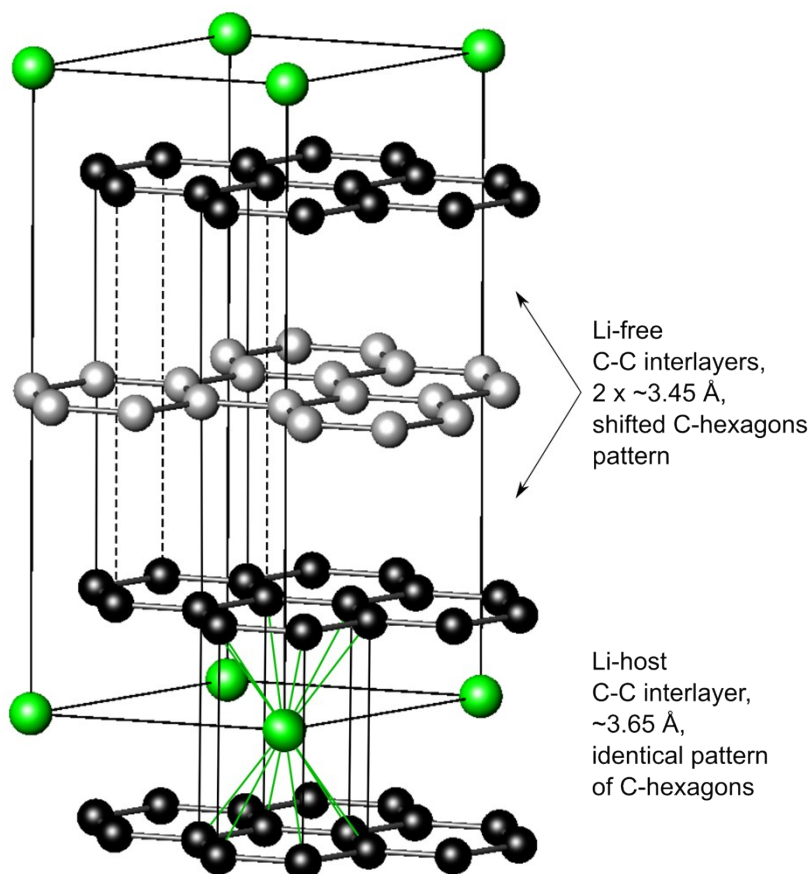
Figure S10. Schematic illustration of the revised crystal structure of LiC$_{18}$ (Stage 3L). In the two smaller C-C interlayer spaces, the central carbon hexagons layer (shown with light-grey spheres) is shifted with respect to the two neighboring layers (black-colored spheres) along, for example, the (100) direction, by exactly the C-C in-plane distance (~1.43 Å). As a result, a half of the carbon atoms in it are located exactly under and above the carbon atoms in the neighboring layers (thin solid vertical lines connecting the light-grey and black atoms). Another half of the light-grey atoms are "seeing" the middles of the hexagons in the layers of the black-colored carbons "above" and "below". Equivalently, for the half of the atoms in the black-colored carbon layers, there is no light-grey colored atom "above" or below them – see the long dashed lines connecting such black atoms through the both shorter C-C interlayers. The second type of interlayer – between the two black-colored layers – features a slightly longer interatomic distance (~3.65 Å), identical atom arrangement in the carbon layers on both sides, and serves as host place for Li atoms. Li atoms are in the 12-fold coordination having a shape of a hexagonal prism.

Table S5 Refined crystal structure parameters of the LiC_{18} phase. All crystallographic sites are fully occupied.

LiC$_{18}$, Space Group P -6 2 m, Z=1, a = 4.2715(3), c = 10.409(1)			
Atom	Wyckoff site		
Li	1a (0,0,0)	$B_{iso,}$ (Å^2)^x	1.5
C1	1b (0,0,1/2);	$B_{iso,}$ (Å^2) ^{xi}	0.60 (3)
C2	3g (x,0,1/2);	x	0.335 (7)
C3	2d (1/3,2/3,1/2);		
C4	6i (x,0,z);	x^{xii}	0.341 (2)
		z^{xii}	0.1777 (2)
C5	6i (x,0,z);	x^{xii}	0.659 (2)
		z^{xii}	0.1777 (2)

----

^{x} B_{iso} value for Li atom was fixed at some reasonable value. The weakness of Li scattering does not allow for a safe refinement of B_{iso} in presence of so many phases.

^{xi} B_{iso} values for all carbon atoms in LiC_{18} were refined with constraint to equality.

^{xii} *a)* In order to keep the layer composed of the C4 and C5 atoms ideally flat, and *b)* in order to preserve the ideal form of hexagons directly hosting the Li site in the middle of the prism between them in the carbon layer, composed of C4 and C5 atoms, the coordinates for these two atoms were refined under such constraints: $x(C4)=-x(C5)$, $z(C4)=z(C5)$.